Altered stability of pulmonary surfactant in SP-C-deficient mice

Stephan W. Glasser*†, Michael S. Burhans*, Thomas R. Korfhagen*, Cheng-Lun Na*, Peter D. Sly‡, Gary F. Ross*, Machiko Ikegami*, and Jeffrey A. Whitsett*

*Division of Pulmonary Biology, Children's Hospital Medical Center, Cincinnati, OH 45229-3039; and ‡Division of Clinical Science, Telethon Institute for Child Health Research, Perth 6872, Australia

Edited by Michael J. Welsh, University of Iowa, College of Medicine, Iowa City, IA, and approved March 19, 2001 (received for review October 20, 2000)

The surfactant protein C (SP-C) gene encodes an extremely hydrophobic, 4-kDa peptide produced by alveolar epithelial cells in the lung. To discern the role of SP-C in lung function, SP-C-deficient (−/−) mice were produced. The SP-C (−/−) mice were viable at birth and grew normally to adulthood without apparent pulmonary abnormalities. SP-C mRNA was not detected in the lungs of SP-C (−/−) mice, nor was mature SP-C protein detected by Western blot of alveolar lavage from SP-C (−/−) mice. The levels of the other surfactant proteins (A, B, D) in alveolar lavage were comparable to those in wild-type mice. Surfactant pool sizes, surfactant synthesis, and lung morphology were similar in SP-C (−/−) and SP-C (+/+) mice. Lamellar bodies were present in SP-C (−/−) type II cells, and tubular myelin was present in the alveolar lumen. Lung mechanics studies demonstrated abnormalities in lung hysteresivity (a term used to reflect the mechanical coupling between energy dissipative forces and tissue-elastic properties) at low, positive-end, expiratory pressures. The stability of captive bubbles with surfactant from the SP-C (−/−) mice was decreased significantly, indicating that SP-C plays a role in the stabilization of surfactant at low lung volumes, a condition that may accompany respiratory distress syndrome in infants and adults.

Pulmonary surfactant is a complex mixture of lipids and proteins that reduces surface tension at the air–liquid interface and prevents alveolar collapse during respiration. Deficiencies of pulmonary surfactant because of premature birth or surfactant inactivation from lung injury can result in a lethal respiratory distress syndrome (RDS). Surfactant replacement by instillation of bovine surfactant extracts has proven effective at treating neonatal RDS (1, 2). Pulmonary surfactant is synthesized and secreted into the alveolar lumen by specialized alveolar type II cells. Four surfactant proteins (SP) with unique properties have been identified in pulmonary surfactant and are termed SP-A, SP-B, SP-C, and SP-D. SP-A and SP-D are relatively hydrophilic proteins and contribute to innate defense of the lung (SP-A, SP-D) (3) and surfactant homeostasis (SP-D) (4). SP-B and SP-C are hydrophobic proteins that enhance surface-active properties of surfactant phospholipid films (5).

Of the surfactant proteins, SP-C is the most hydrophobic. The alveolar form of SP-C is a 34- to 35-aa peptide that is proteolytically processed from a 21-kDa precursor protein (5). The sequence of the SP-C peptide is highly conserved among mammalian species. The extremely hydrophobic properties of SP-C are a result of a valine-rich region within an extended 23-aa hydrophobic domain from residues 13–35. Nineteen of these 23 aa are valine, leucine, or isoleucine. This hydrophobic domain forms an α-helical structure with the α-helix capable of spanning a lipid bilayer. The hydrophobicity of SP-C is augmented further by palmitoylation of two amino-terminal cysteine residues located at positions 5 and 6 (5, 6). Together, these features account for the strong association of SP-C with surfactant phospholipids.

SP-C expression is initiated early in the embryonic period of lung formation, wherein SP-C transcripts are detected uniformly in epithelial cells lining the primitive airways. As the branching tubules elongate, SP-C expression is decreased in cells of the proximal conducting portion of the lung and maintained in epithelial cells in the periphery of the developing respiratory tubules (7). Ultimately, the respiratory tubules form alveoli and SP-C mRNA is detected only in alveolar type II cells of the mature lung (7).

Surfactant preparations containing phospholipids and SP-C are highly surface active *in vitro* (8, 9). Surfactant replacement with phospholipid preparations enriched in SP-C are highly effective in treatment of respiratory distress (1). Bovine surfactant preparations presently in clinical use contain phospholipids and are enriched in SP-C (8). A synthetic surfactant composed of dipalmitoyl-phosphatidylcholine, phosphatidylglycerol, and recombinant human SP-C restored lung compliance in premature sheep, rabbit, and adult animal models of acute lung injury (10–14). SP-C-based surfactant presently is being evaluated in clinical studies for the treatment of adult respiratory distress syndrome. Although *in vitro* and *in vivo* studies indicate that SP-C contributes to surfactant function, whether SP-C is required for or contributes to surfactant function *in vivo* has not been determined. To discern the role of SP-C in the lung, we have inactivated the SP-C gene in embryonic stem (ES) cells to produce mice lacking SP-C.

Materials and Methods

Vector Construction. A 129/J mouse genomic library was screened to identify genomic clones of the SP-C gene homologous to the 129 derived ES cells. A 2.1-kb *Bam*HI fragment containing exons 2–6 of the SP-C gene was used for modification of the gene. Sequence encoding the hydrophobic polyvaline domain of the SP-C peptide was interrupted by insertional mutagenesis with a 1.6-kb pGKneo gene cassette. This insertion provided positive selection for targeted cells by growth in the neomycin analogue G418. The 2.1-kb SP-C plasmid was digested with *Apa*LI, which cuts at a unique *Apa*LI site located in the SP-C polyvaline domain. The *Apa*LI linker pGKneoBPA cassette was ligated into the SP-C *Apa*LI site. A 1.3-kb *Pst*I-to-*Bam*HI fragment spanning exon 1 and the 5′ flanking DNA was ligated to the 5′ *Bam*HI site of the 2.1-kb Bam-pGKneoBPA fragment. The targeting construct was modified further by cloning the herpes simplex virus thymidine kinase gene into the 5′ *Sph*I site to provide gancyclovir selection against nonhomologous integration of the construct.

Generation of SP-C Null Mutant Mice. The D3R strain of ES cells (kind gift of Thomas Doetschman and John Duffy, University of

This paper was submitted directly (Track II) to the PNAS office.

Abbreviations: SP-C, surfactant protein C; RDS, respiratory distress syndrome; ES, embryonic stem; RT, reverse transcription; Sat PC, saturated phosphatidylcholine; PEEP, positive end-expiratory pressure.

†To whom reprint requests should be addressed at: Children's Hospital Medical Center, Division of Pulmonary Biology, 3333 Burnet Avenue, Cincinnati, OH 45229-3039. E-mail: glass0@chmcc.org.

The publication costs of this article were defrayed in part by page charge payment. This article must therefore be hereby marked "*advertisement*" in accordance with 18 U.S.C. §1734 solely to indicate this fact.

 www.pnas.org/cgi/doi/10.1073/pnas.101500298

Cincinnati) was electroporated with the purified SP-C-targeting construct DNA and selected as described (15). ES cell DNA was digested with *Bsu*36I and analyzed with a probe outside of the targeting construct sequence. The probe was a 457-bp *Sph*I-*Pst*I fragment adjacent to the 5′ limit of the targeting construct. Positive clones were confirmed by genomic Southern blot of multiple restriction enzyme digests.

ES cell clones carrying a targeted SP-C allele were microinjected into C57/Bl6 blastocysts and implanted into host mice. Chimeric offspring were identified by mosaic Agouti coat color and bred to NIH Swiss black (Tac:N:NIHSBCfBr from Taconic Farms) females. Agouti offspring were screened for germ-line transmission of the targeted SP-C allele by genomic Southern blot analysis of *Bgl*II- and *Sph*I-digested tail DNA. The 5′ Sph-Pst fragment was used as a probe. The F1 offspring heterozygous for the SP-C mutation (+/−) were bred to establish a colony of SP-C (+/+), SP-C (+/−), and SP-C (−/−) mice. All mice were maintained in a pathogen-free barrier containment facility with filtered air, water, and autoclaved food.

Analysis of RNA and Protein Expression. Lung RNA was extracted from the lungs of adult SP-C (+/+), (+/−), and (−/−) mice by tissue homogenization in 4 M guanidinium isothiocyanate solution and centrifuge separation by using phase-lock gels as recommended (5′ → 3′). Ten micrograms of total lung RNA from each genotype was separated by agarose gel electrophoresis and transferred to nylon membranes for hybridization analysis. Membranes were probed with either murine SP-B or murine SP-C cDNA clones as described (15). The relative abundance of mRNA species were quantitated by using a PhosphorImager and IMAGEQUANT software (Molecular Dynamics). Analysis of the minor SP-C RNA species detected by Northern blot analysis was characterized further using by exon-specific PCR analysis of cDNA generated by reverse transcription (RT) of lung RNA. RT cDNA derived from lung RNA of SP-C (−/−) mice was subject to 25 cycles of PCR amplification with an exon 1-specific 5′ primer and an exon 4- or exon 5-specific 3′ primer (5′ exon 1 primer: TCT TGA TGG AGA CTC CAC CG; 3′ exon 4 primer: CTG GCT TAT AGG CCG CTA GG; 3′ exon 5 primer: TCC GAT GCT CAT CTC AAG GA).

Detection of Alveolar Surfactant Proteins by Western Blot Analysis. Surfactant protein in alveolar lavage was separated by SDS/PAGE on 10–20% Tricine gels, and samples were normalized to 2 μg of saturated phosphatidylcholine (Sat PC) and loaded onto the gel for immunoblot analysis. The primary antibody was a rabbit antirecombinant SP-C serum that was used at a dilution of 1:25,000. The high-titer anti-SP-C antibody was raised against a modified human recombinant, 34-aa SP-C peptide (provided by Byk-Gulden Pharmazeutika). The specificity of the antibody for the mature form of SP-C was characterized (16). Western blot analysis of alveolar lavage proteins was performed with polyclonal antibodies to SP-A, SP-B, and SP-D as described (17).

Lung Morphology and Ultrastructure. Lung morphology was visualized by conventional histological staining of paraffin-embedded tissue, and type II cells were visualized by immunostaining with an antibody specific to SP-B (15). Lungs from three SP-C (−/−) and SP-C (+/+) 8-week-old mice were collected after inflation fixation and prepared for electron microscopy as described (17).

Sat PC Pool Sizes and Precursor Incorporation into Sat PC. The amount of Sat PC in lipid extracts of alveolar lavage and lung tissue after alveolar lavage from 8-week-old mice ($n = 8$ for each group) was determined as described (4), as was the incorporation rate of [^{3}H]choline into Sat PC.

Surface Activity of Surfactant. Large aggregate surfactant was isolated from alveolar lavages by centrifugation at 40,000 × *g* for 15 min over 0.8 M sucrose in 0.9% NaCl cushion. The large aggregate surfactant was recovered from the sucrose interface. The surface activity of three pools (three mice per pool) of isolated large aggregate for each genotype group was measured with a captive bubble surfactometer. The concentration of each sample was adjusted to 3 nmol Sat PC/μl in 0.9% NaCl, and 3 μl of the surfactant was applied to the air–water interface of a 23.1 ± 0.9 μl bubble at 37°C. The surface tension was measured every 10 sec, equilibrium surface tension was measured at 60 sec, and bubble pulsation was started (4). The minimum surface tensions after 65% volume reduction of the bubbles were measured for the fifth pulsation. To test the ability of isolated surfactant to stabilize small bubbles, 3 μl of 0.3 nmol Sat PC/μl large aggregate surfactant was applied to the air–water interface and the bubble was adjusted to a 1.3 ± 0.1 μl volume; surface tension was measured for 12 min. From the calculation of bubble surface areas, it was determined that 10 times less Sat PC would maintain a similar surfactant concentration to surface area for the smaller-size bubble.

Lung Mechanics. For lung mechanics studies, mice were anesthetized with 0.1 ml/10 g of a mixture containing xylazine (2.0 mg/ml) and ketamine (40 mg/ml). Two-thirds of the dose was given to induce anesthesia, with the remaining given when the animals were attached to the ventilator. A tracheostomy was performed and a polyethylene cannula (1.0 cm, i.d. = 0.023 cm) was inserted. Mice were ventilated with a tidal volume of 8 ml/kg at a rate of 450 breaths per minute, with a positive end-expiratory pressure (PEEP) of 0, 1, 2, and 4 cm H_2O, using a custom-designed ventilator (flexiVent; Scireq, Montreal). This ventilator allowed us to measure lung function by using a modification of the low-frequency forced oscillation technique. Respiratory input impedance was measured between 0.25 and 20 Hz by applying a composite signal containing 19 mutually prime sinusoidal waves during pauses in regular ventilation. For each measurement, the ventilator was paused for 1 sec with the mouse exposed to the desired PEEP level, ensuring the appropriate end-expiratory pressure. The expiratory valve then was closed and the oscillatory-forcing function was applied by the piston. As the mouse was exposed to a closed system during the measurements, changes in lung volume were avoided. The constant-phase model described by Hantos *et al.* (18) was used to partition respiratory input impedance into components representing the mechanical properties of the airway resistance and a constant-phase tissue component (Gtissue-Htissue)/w^{α}, where Gtissue and Htissue are coefficients for tissue resistance and tissue elastance, w is the angular frequency, and α determines the frequency dependence of the real and imaginary parts of the impedance. Hysteresivity describes the mechanical coupling between tissue resistance, and elastance and is calculated as Hysteresivity = Gtissue/Htissue. The calibration procedure removes the impedance of the equipment and tracheal tube. The results reported represent the mechanical properties of the mice alone.

Results

SP-C Null Mutant Mice. Five ES colonies were identified that carried the correctly targeted SP-C allele (Fig. 1 *A* and *B*). Three of the ES clones were microinjected into mouse blastocysts that produced 34 chimeric mice. Chimeric males were bred to NIH Swiss black mice. Germ-line transmission to F1 offspring was identified by Southern blot analysis of *Bgl*II-digested DNA by using the same 5′ probe with which the 5.7-kb *Bgl*II band increased to 7.4 kb. Germ-line transmission of the modified SP-C allele was detected in offspring of chimeric mice generated from each of the three injected ES cell clones. F1 offspring heterozy-

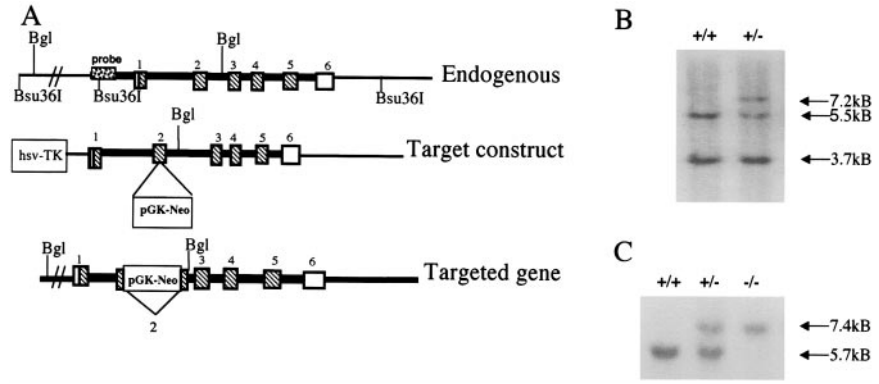

Fig. 1. SP-C targeting construct and Southern blot identification of targeted ES cells and mice. (*A*) A restriction map of the SP-C gene is shown above the targeting vector. Exons are numbered 1–6. The bottom line diagrams the targeted SP-C gene. Precise homologous recombination between lines 1 and 2 results in exon 2 interrupted by the neomycin resistance (pGKneo) gene and loss of the nonhomologous herpes simplex virus thymidine kinase (HSV-TK) gene (bottom line). (*B*) Southern blot analysis of *Bsu*36I genomic DNA from ES cells. *Bsu*36I-digested DNA was probed with a 5′ Sph-Pst fragment adjacent to the targeting DNA, which detects 3.7-kb upstream and 5.5-kb downstream endogenous bands (+/+, lane 1). DNA from a targeted ES cell colony (+/−) shows the 5.5-kb allele and the targeted allele that are increased by the size of the inserted pGKneo cassette to 7.2 kb. (*C*) Southern blot analysis of genomic DNA from SP-C gene-targeted mice. The 5′ probe was used for blots of *Bgl*II-digested DNA. A single, 5.7-kb *Bgl*II band is detected in wild-type mice by the 5′ probe. Two bands are detected in mice heterozygous for the targeted site (+/−). Homozygous SP-C (−/−) mice produce only the 7.4-kb, larger upper band, indicating that both SP-C alleles are interrupted.

gous for the targeted SP-C allele were bred to produce SP-C (+/+), (+/−), and (−/−) mice (Fig. 1*C*). The SP-C (−/−) mice were viable at birth and were similar to normal littermates in growth and reproduction. SP-C (−/−) mice have been maintained for eight generations in the vivarium.

SP-B and SP-C mRNA and Protein Levels. SP-C and SP-B mRNA was assessed by Northern blot analysis of lung RNA from SP-C (+/+), (+/−), and (−/−) mice. SP-C mRNA levels in lungs from SP-C (+/−) mice were approximately half the level (63%) of SP-C (+/+) mice. No mature SP-C mRNA was detected in SP-C (−/−) mice (Fig. 2*A*). A faint band of hybridization smaller than the SP-C mRNA was detected in lungs from SP-C (−/−) mice. This mRNA species was present at ≈1% of the wild-type SP-C mRNA. Lung RNA was converted to cDNA for RT-PCR analysis to determine the size and sequence of the minor band. RT-PCR analysis of SP-C (−/−) lung RNA by using an exon 1 primer coupled with exon 4 or 5 downstream primers produced single bands that were consistent with an SP-C cDNA product wherein exon 2 was absent. Sequence of the PCR products confirmed SP-C sequence that was a direct splice from the end of exon 1 to the start of exon 3 (data not shown). Thus, the minor SP-C mRNA species found by Northern blot in SP-C (−/−) mice is an alternate splice eliminating exon 2 and the encoded mature airway peptide. No band corresponding to the full-length SP-C product was detected. SP-B mRNA expression was unaltered in SP-C (+/−) or SP-C (−/−) mice (Fig. 2*A*).

Consistent with the Northern blot data, mature SP-C protein was not detected in alveolar lavage from SP-C (−/−) mice, whereas the mature SP-C peptide was readily detected by Western blot of alveolar lavage from wild-type SP-C (+/+) and SP-C (+/−) mice (Fig. 3*A*). Densitometric quantitation of the SP-C (+/+) and (+/−) bands indicated that in the (+/−)

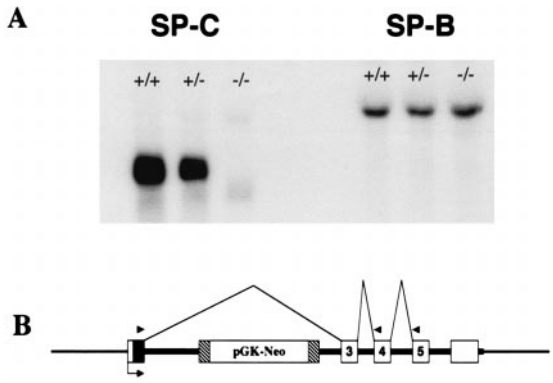

Fig. 2. Northern blot analysis of RNA from the lungs of SP-C (+/+), (+/−), and (−/−) mice. Total RNA was separated by gel electrophoresis, and blots were probed with an SP-C cDNA probe (*Left*) or SP-B cDNA probe (*Right*). An SP-C band of ≈900 bp was detected in (+/+) mice. Reduced SP-C hybridization was detected in (+/−) lung RNA. No full-length SP-C mRNA was detected in the (−/−) lung RNA, whereas a smaller minor band was detected that lacks the SP-C coding sequences of exon 2. The alternate splicing of the disrupted gene is diagrammed below the blot (*B*).

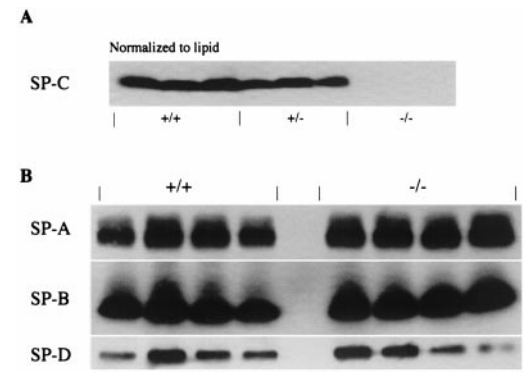

Fig. 3. Surfactant protein levels in alveolar lavage of SP-C-targeted mice. Alveolar lavage containing the pulmonary surfactant was collected from SP-C (+/+), (+/−), and (−/−) mice. Samples were normalized to saturated phosphatidylcholine and resolved by SDS/PAGE followed by immunoblot analysis with a polyclonal antibody specific to each surfactant protein. (*A*) Levels of mature SP-C were assessed with an antibody specific to recombinant SP-C peptide. SP-C (+/+) lavage samples were run in lanes 1–3, SP-C (+/−) samples were run in lanes 4–6, and SP-C (−/−) samples were run in lanes 7–9. The amount of mature SP-C peptide is reduced in the SP-C (+/−) mice by approximately half and is entirely absent in the SP-C (−/−) lanes. (*B*) Abundance of the other three surfactant proteins was evaluated in lung lavage from SP-C (+/+) and SP-C (−/−) mice. Immunoblots of lavage samples are shown for SP-A (*Top*), SP-B (*Middle*), and SP-D (*Bottom*). Lanes 1–4 are from SP-C (+/+) mice and lanes 5–8 are from SP-C (−/−) mice.

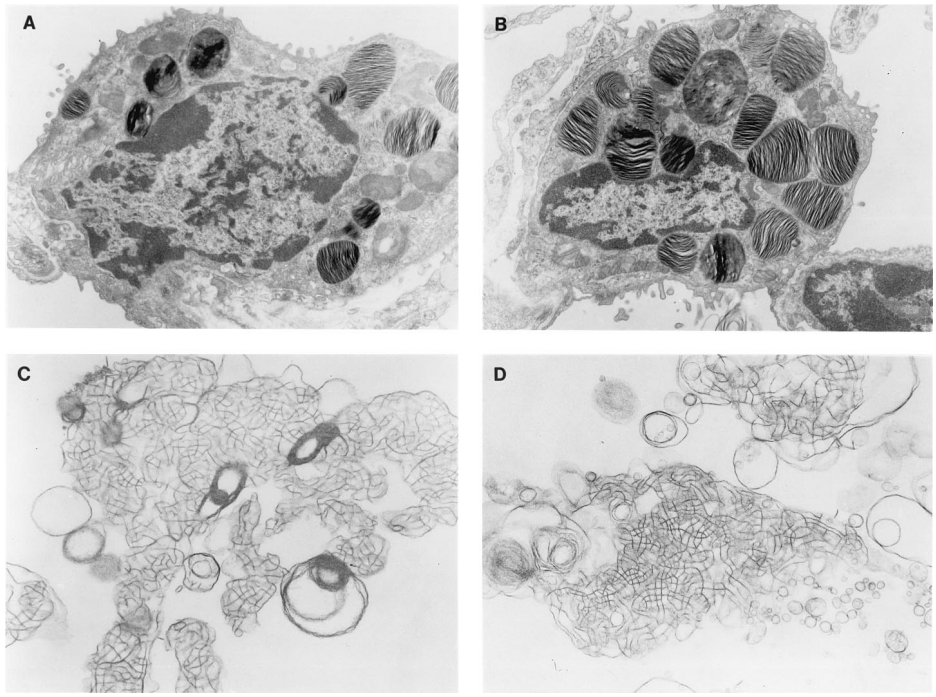

Fig. 4. Ultrastructure of type II epithelial cells in SP-C-deficient mice. Lung tissue from adult mice was prepared for electron microscopy. Intact lamellar bodies (intracellular form of surfactant) were detected in SP-C (+/+) type II cells (*A*) and in SP-C (−/−) type II cells (*B*), ×10,400. Extracellular tubular myelin forms of surfactant were detected in SP-C (+/+) mice (*C*) and SP-C (−/−) mice (*D*), ×26,000.

mice, SP-C peptide was present at 60% of the SP-C level in SP-C (+/+) mice. This result was consistent with SP-C expression from a single allele in the (+/−) mice. The mature form of the SP-B protein was present in alveolar lavage of SP-C (−/−) mice equivalent to SP-B levels in SP-C (+/+) mice (Fig. 3*B*). The concentrations of surfactant proteins SP-A and SP-D showed modest differences (Fig. 3*B*). Quantitative values for SP-B in SP-C (−/−) mice were 0.89 ± 0.25 relative to SP-C (+/+) mice, with SP-B levels set to a valve of 1 ± 0.36. The SP-A value in SP-C (−/−) mice was 1.34 ± 0.18 of SP-C (+/+) mice, and the SP-D value in SP-C (−/−) mice was 0.84 ± 0.44 of the SP-D in SP-C (+/+) mice. Collectively, the Western blot analysis for SP-A, SP-B, and SP-D indicates that concentrations of these surfactant proteins were not influenced by SP-C and that these surfactant proteins are regulated independent of SP-C.

Lung Morphology. Morphology of lung tissue from SP-C (−/−) mice was indistinguishable from the SP-C (+/−) or wild-type mice. Alveolar and bronchiolar structures were normal with no indications of inflammation. The number of type II cells appeared equivalent in SP-C (−/−) and (+/+) mice (data not shown). The lungs of SP-C (−/−), (+/−), and (+/+) mice were examined by electron microscopy to determine whether the elimination of SP-C altered type II cell morphology or intra- and extracellular forms of pulmonary surfactant. In adult SP-C (−/−) mice, numerous mature well organized lamellar bodies (the intracellular form of surfactant) were detected in type II cells of both SP-C (−/−) and SP-C (+/+) mice (Fig. 4 *A* and *B*). Fusion of multivesicular bodies to form lamellar bodies was observed in SP-C (−/−) mice. Extracellular tubular myelin forms of pulmonary surfactant were readily detected in micrographs of the alveoli from SP-C (−/−), (+/−), and (+/+) mice (Fig. 4 *C* and *D*). The size and abundance of lamellar bodies were assessed by electron microscopy and were unaltered (data not shown).

Sat PC Pool Sizes and Precursor Incorporation into Sat PC. Surfactant Sat PC pool size in alveolar lavage and total lung (alveolar lavage plus lung tissue after lavage) were similar in SP-C (−/−) and SP-C (+/+) mice. The alveolar Sat PC was 10.7 ± 0.5 μmol/kg for SP-C (−/−) mice and 9.7 ± 0.5 μmol/kg for SP-C (+/+) mice. Total lung Sat PC was 31.9 ± 1.4 μmol/kg for SP-C (−/−) mice and 31.2 ± 1.1 μmol/kg for SP-C (+/+) mice. [^{3}H]Choline incorporation into alveolar lavage Sat PC of SP-C (−/−) mice was 615 ± 49 cpm and 681 ± 49 cpm for SP-C (+/+) mice. Incorporation into total lung Sat PC was 2,575 ± 157 cpm for SP-C (−/−) mice and 2,314 ± 169 cpm for SP-C (+/+) mice. The secretion rate of Sat PC was 21.4 ± 1.3% in SP-C (−/−) mice and 25.2 ± 1.5% in SP-C (+/+) mice, and no significant differences were detected between the groups. Thus, lack of SP-C does not alter surfactant synthesis rate, secretion rate, or the surfactant pool size.

Surface Activity of Surfactant and Lung Mechanics. Measurements made at increasing end-expiratory pressures from 0 to 4 cm H_2O showed no significant changes in airway resistance, Gtissue, and Htissue between SP-C (+/+) and SP-C (−/−) mice. However, statistically significant lower hysteresivity was seen in all SP-C (−/−) mice at each end-expiratory pressure, indicating reduced viscoelasticity of the lungs of SP-C (−/−) mice (Fig. 5).

When using captive-bubble surfactometry with a standard size bubble (23 μl), the surface activity of large aggregate surfactant isolated from SP-C (−/−) mice was normal and showed equilibrium surface tension and minimum surface tension similar to that from SP-C (+/+) mice (Fig. 6*A*). The difference in altered hysteresivity was considered to reflect altered surfactant activity at low-end expiration or small alveolar volumes. Therefore, the surface tension of surfactant from SP-C (+/+) and (−/−) mice was evaluated *in vitro* by using a minimal-size bubble (1.3 μl) in the captive-bubble surfactometer to assess surfactant activity in bubbles with small radii. Stability of small bubbles was decreased markedly with the SP-C (−/−) surfactant, whereas equilibrium

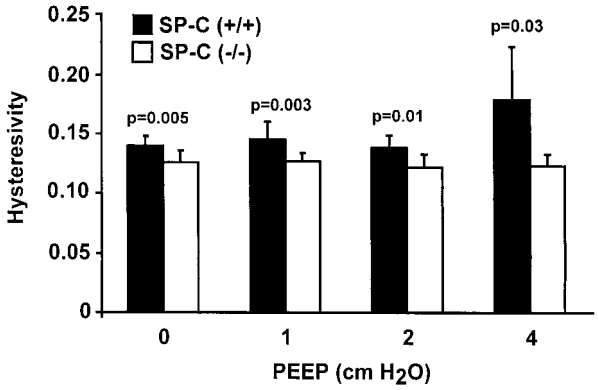

Fig. 5. Lung mechanics. Hysteresivity, which is the viscoelasticity of the lung tissue, was calculated as Gtissue/Htissue at PEEP of 0, 1, 2, and 4 cm H_2O. Hysteresivity was significantly lower for SP-C (−/−) mice than SP-C (+/+) mice overall (ANOVA, $P < 0.05$) and for each value of PEEP (*P* values shown in figure). Data shown are group mean and SD.

surface tension was unaltered with surfactant from SP-C (+/+) mice ($n = 4$ measurements). The changes in surface tension are shown in Fig. 6*B*. The results are consistent with a role for SP-C in stabilization of phospholipid packing at small bubble radius and facilitation of the recruitment of phospholipids from the subphase to the surface film.

Discussion

The mouse SP-C gene was inactivated by gene targeting. The lungs of the SP-C (−/−) mice lack detectable mature SP-C or precursor SP-C (proSP-C). In the absence of detectable SP-C, these mice survive and grow normally with no adverse effects on health, reproduction, or pulmonary function. SP-B mRNA levels and the level of SP-A, SP-B, and SP-D proteins were unaltered in the alveolar lavage of SP-C (−/−) mice. Both SP-C and SP-B are hydrophobic peptides that dramatically enhance surface activity of surfactant phospholipids. The survival of the SP-C (−/−) mice in the absence of the mature active SP-C peptide indicates that SP-C is not required for the surface properties of the alveolar phospholipid films required for respiratory function *in vivo*. However, subtle abnormalities in lung mechanics and the instability of SP-C (−/−) surfactant at low bubble size support the importance of SP-C in surfactant function at low lung volumes such as that seen in respiratory distress syndrome in adults and preterm infants. The present findings in the SP-C (−/−) mice are distinct from results reported for SP-B gene-targeted mice and infants with hereditary SP-B deficiency, wherein severe respiratory failure occurs at birth (15, 19). In the SP-B (−/−) mice and human infants with hereditary SP-B deficiency, the mature form of SP-C was absent or diminished and an aberrant form of proSP-C was detected.

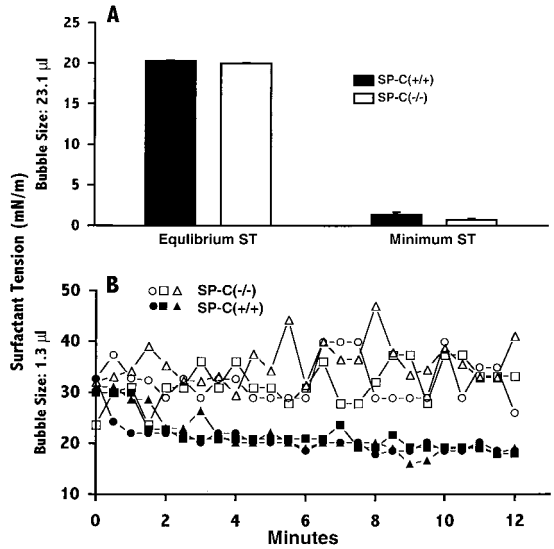

Fig. 6. Surfactant function. Three pools of large aggregate fractions (three mice/pool) of surfactant from SP-C (+/+) and SP-C (−/−) mice were used to assess equilibrium surface tension, and minimal surface tension was achieved on a captive-bubble surfactometer. The equilibrium surface tension and minimum surface tension were measured by using a standard bubble size (*A*). Surface tension measurements with a reduced bubble volume (*B*) demonstrated bubble-surface film instability with surfactant preparation from SP-C (−/−) mice whereas bubble stability was maintained with surfactant preparations from SP-C (+/+) mice.

Histological analysis of lungs from SP-C (−/−) mice demonstrated normal morphogenesis of the conducting and peripheral airways. Alveolar structure was unaltered with a normal distribution of type II cells (SP-B-positive) throughout the parenchyma with normal surfactant lipid pool sizes in SP-C (−/−) mice. Radiolabeled choline incorporation into Sat PC by lungs of SP-C (−/−) mice was similar to that in SP-C (+/+) mice, indicating that SP-C is not essential for the synthesis or secretion of pulmonary surfactant.

Lamellar bodies and tubular myelin, the unique intracellular and extracellular forms of pulmonary surfactant, respectively, were unaltered in SP-C (−/−) mice. In contrast, alterations in intra- and extracellular forms of surfactant were detected when SP-A, SP-B, and SP-D genes were targeted (17, 15, 20, 21). Pulmonary surfactant is synthesized in type II cells and routed to multivesicular bodies, which subsequently fuse to form the distinctive lamellar bodies that serve as the presecretory storage form of surfactant. Upon secretion, lamellar bodies form an extracellular reservoir of surfactant termed tubular myelin. All of these structures were present in type II cells and air spaces of SP-C (−/−) mice. This observation is distinct from those in SP-B (−/−) mice, wherein enlarged multivesicular bodies were observed in type II cells but no lamellar bodies were detected (15). The aberrant lipid inclusions seen in SP-B (−/−) animals are attributed in part to incorrect vesicle fusion, which is mediated by SP-B. In SP-A (−/−) mice, normal lamellar bodies were detected whereas the extracellular tubular myelin forms of surfactant were virtually absent. SP-D (−/−) mice had an increased surfactant phospholipid pool size and corresponding increase in the size of lamellar bodies in type II cells (20, 21). The current findings indicate that loss of SP-C is not required for formation of lamellar bodies or tubular myelin structures.

SP-C has been hypothesized to play an important role in surfactant function based on the ability of SP-C to enhance phospholipid surface activity *in vitro* and to restore compliance in surfactant-deficient immature rabbit and depleted animal lung models. Instillation of SP-C preparations into the lungs of preterm rabbits and lambs improved lung pressure volume curves and lung compliance (11). Similarly, SP-C-based synthetic surfactants improved lung compliance and oxygenation in adult rat and sheep lung injury models (12–14). When measurements of lung mechanics were evaluated at end expiration (low PEEP), the SP-C (−/−) mice had only modest increases in airway and tissue resistance, whereas hysteresivity was reduced significantly in these animals. A major function of surfactant is to reduce surface tension in the alveoli as the lung volume decreases. This lowering of surface tension at low lung volumes prevents airway collapse at end expiration. Surfactant function is perhaps less important at high lung volumes, where the collagen and elastin fiber network have more influence on limiting lung inflation. The present finding, demonstrating decreased hysteresivity at

low PEEP pressures, suggests that SP-C may stabilize phospholipid films at reduced lung volumes.

Phospholipid mixtures supplemented with purified SP-C or rSP-C or SP-B were more effective in restoring lung compliance of premature rabbit pups when ventilated with a PEEP of 4 cm H_2O, similar to the conditions used in the analysis of the hysteresivity of lungs from SP-C (−/−) mice (22). Surfactant films lacking SP-C were unstable in small, captive bubbles compared with the stability of surfactant preparations containing SP-C. This difference in stability was detected only in bubbles with small radii wherein phospholipid packing is high. Ultrastructural analysis of surfactant films *in vitro* demonstrates the presence of both monolayers and multilayers of phospholipids, the latter being evident when surfactant films are highly compressed (23). Analysis of the alveolar surfactant film structure by electron microscopy demonstrates that the surface film contains regions of multilamellar stacks *in vivo* that are similar to those found *in vitro* (24). We hypothesize that SP-C may stabilize adjacent lipid layers that form during film compression and promote formation of surfactant reservoirs that maintain availability of phospholipids for surface tension reduction at the air–liquid interface. Both SP-C and SP-B enhance the rate of surfactant film formation as phospholipids move onto an expanding surface. However, SP-C-deficient surfactant is uniquely unstable at low bubble volumes that also have a high angle of curvature, perhaps leading to the instability of films seen in the captive-bubble assay. These biophysical properties of SP-C-deficient surfactant are also consistent with the loss of hysteresivity at low lung volumes seen during forced oscillatory ventilation of SP-C (−/−) mice. Present findings in SP-C (−/−) mice are consistent with previous work demonstrating that SP-C (*i*) enhances the rate of film formation, perhaps by contributing to regional differences in phospholipid packing in membranes, and (*ii*) partitions into and perhaps stabilizes densely packed gel phase phospholipids, such as dipalmitoyl-phosphatidylcholine (25, 26). Despite the changes in lung mechanics and surfactant activity, pulmonary function is remarkably normal in SP-C gene-targeted mice.

The instability of SP-C-deficient surfactant and decreased hysteresivity at low lung volumes predicts that under physiologic stress, SP-C deficiency may lead to alveolar instability that may contribute to the pathogenesis of respiratory distress syndromes. SP-C gene expression is inhibited after infection and exposure to tumor necrosis factor α and is decreased in lungs of infants with respiratory distress syndrome, pneumonia, and pulmonary edema (27, 28). Although SP-C is not required for normal pulmonary mechanics at normal lung volumes, decreased surfactant proteins or phospholipids caused by injury or infection may cause surfactant dysfunction, leading to alveolar instability or acute alveolar collapse as seen in RDS, adult respiratory distress syndrome, or pneumonia. Indeed, recent studies identified subsets of children with selective deficiency of SP-C that developed severe acute (29) and chronic lung disease in infancy (R. S. Amin, S. E. Wert, R. P. Baughman, J. F. Tomashefski, L. M. Nogee, A. S. Brody, W. M. Hull, and J.A.W., unpublished results; ref. 30).

We acknowledge the efforts of Dr. Karen Yager and Sandy Falcone of the Transgenic Core Facility of the Children's Hospital Research Foundation for the blastocyst injections, Drs. John Baatz and Timothy Weaver for helpful discussions, and Ms. Ann Maher for assistance in manuscript preparation. This work was supported by National Heart, Lung, and Blood Institute Grants HL50046 (to S.W.G.), PPG HL61646 (to S.W.G., T.R.K., M.I., and J.A.W.), and HL38865 (to J.A.W.).

1. Jobe, A. H. (1993) *N. Engl. J. Med.* **328,** 861–868.
2. Creuwels, L. A. J., vanGolde, L. M. G. & Haagsman, H. P. (1997) *Lung* **175,** 1–39.
3. Mason, R. J., Greene, K. & Voelker, D. R. (1998) *Am. J. Physiol.* **275,** L1–L13.
4. Ikegami, M., Whitsett, J. A., Jobe, A., Ross, G., Fisher, J. & Korfhagen, T. (2000) *Am. J. Physiol.* **279,** L468–L476.
5. Weaver, T. E. (1998) *Biochim. Biophys. Acta* **1408,** 173–179.
6. Johansson, J. (1998) *Biochim. Biophys. Acta* **1408,** 161–172.
7. Wert, S. E., Glasser, S. W., Korfhagen, T. R. & Whitsett, J. A. (1993) *Dev. Biol.* **156,** 426–443.
8. Whitsett, J. A., Ohning, B. L., Ross, G., Meuth, J., Weaver, T., Holm, B. A., Shapiro, D. L. & Notter, R. H. (1986) *Pediatr. Res.* **20,** 460–467.
9. Yu, S. H. & Possmayer, F. (1990) *Biochim. Biophys. Acta* **1046,** 233–241.
10. Hawgood, S., Ogawa, A., Yukitake, K., Schlueter, M., Brown, C., White, T., Buckley, D., Lesikar, D. & Benson, B. (1996) *Am. J. Respir. Crit. Care Med.* **154,** 484–490.
11. Davis, A. J., Jobe, A. H., Hafner, D. & Ikegami, M. (1998) *Am. J. Respir. Crit. Care Med.* **157,** 553–559.
12. Hafner, D., Germann, P. G. & Hauschke, D. (1998) *Am. J. Respir. Crit. Care Med.* **158,** 270–278.
13. Lewis, J., McCaig, L., Hafner, D., Spragg, R., Veldhuizen, R. & Kerr, C. (1999) *Am. J. Respir. Crit. Care Med.* **159,** 741–747.
14. Spragg, R. G., Smith, R. M., Harris, K., Lewis, J., Hafner, D. & Germann, P. (2000) *J. Appl. Physiol.* **88,** 674–681.
15. Clark, J. C., Wert, S. E., Bachurski, C. J., Stahlman, M. T., Stripp, B. R., Weaver, T. E. & Whitsett, J. A. (1995) *Proc. Natl. Acad. Sci. USA* **92,** 7794–7798.
16. Ross, G. F., Ikegami, M., Steinhilber, W. & Jobe, A. H. (1999) *Am. J. Physiol.* **277,** L1104–L1108.
17. Korfhagen, T. R., Bruno, M. D., Ross, G. F., Huelsman, K. M., Ikegami, M., Jobe, A. H., Wert, S. E., Stripp, B. R., Morris, R. E., Glasser, S. W., *et al*. (1996) *Proc. Natl. Acad. Sci. USA* **93,** 9594–9599.
18. Hantos, Z., Daroczy, B., Suki, B., Nagy, S. & Fredberg, J. J. (1992) *J. Appl. Physiol.* **72,** 168–178.
19. Nogee, L. M., deMello, D. E., Dehner, L. P. & Colten, H. R. (1993) *New Engl. J. Med.* **328,** 406–410.
20. Botas, C., Poulain, F., Akiyama, J., Brown, C., Allen, L., Goerke, J., Clements, J., Carlson, E., Gillespie, A. M., Epstein, C., *et al.* (1998) *Proc. Natl. Acad. Sci. USA* **95,** 11869–11874.
21. Korfhagen, T. R., Sheftelyevich, V., Burhans, M. S., Bruno, M. D., Ross, G. F., Wert, S. E., Stahlman, M. T., Jobe, A. H., Ikegami, M., Whitsett, J. A., *et al.* (1998) *J. Biol. Chem.* **273,** 28438–28443.
22. Davis, A. J., Jobe, A. H., Häfner, D. & Ikegami, M. (1998) *Am. J. Respir. Crit. Care Med.* **157,** 553–559.
23. Galla, H. J., Bourdos, N., VonNaheman, A., Amrein, M. & Sieber, M. (1998) *Thin Solid Films* **327–329,** 632–635.
24. Schurch, S., Green, F. H. & Bachofen, H. (1998) *Biochem. Biophys. Acta* **1408,** 180–202.
25. Horowitz, A. D., Elledge, B., Whitsett, J. A. & Baatz, J. E. (1992) *Biochim. Biophys. Acta* **1107,** 44–54.
26. Horowitz, A. D., Baatz, J. E. & Whitsett, J. A. (1993) *Biochemistry* **32,** 9513–9523.
27. Wispé, J. R., Clark, J. C., Warner, B. B., Fajardo, D., Hull, W. M., Holtzman, R. B. & Whitsett, J. A. (1990) *J. Clin. Invest.* **86,** 1954–1960.
28. Khoor, A., Stahlman, M. T., Gray, M. E. & Whitsett, J. A. (1994) *J. Histochem. Cytochem.* **42,** 1187–1199.
29. Wert, S. E., Profitt, S. A., Whitsett, J. A. & Nogee, L. M. (1998) *Am. J. Respir. Crit. Care Med.* **157,** A698.
30. Nogee, L. M., Dunbar, A. E., Wert, S. E., Askin, F., Hamvas, A. & Whitsett, J. A. (2001) *N. Engl. J. Med.* **344,** 573–579.